

## Supporting information

### **Synergistic antitumor efficacy of hybrid micelles with mitochondrial targeting and stimuli-responsive drug release**

Zhoujiang Chen,<sup>a,b</sup> Zhanlin Zhang,<sup>a</sup> Maohua Chen, Songzhi Xie,<sup>a</sup> Tao Wang,<sup>a</sup> Xiaohong Li<sup>a,\*</sup>

<sup>a</sup> *Key Laboratory of Advanced Technologies of Materials, Ministry of Education, School of Materials Science and Engineering, Southwest Jiaotong University, Chengdu 610031, P.R. China*

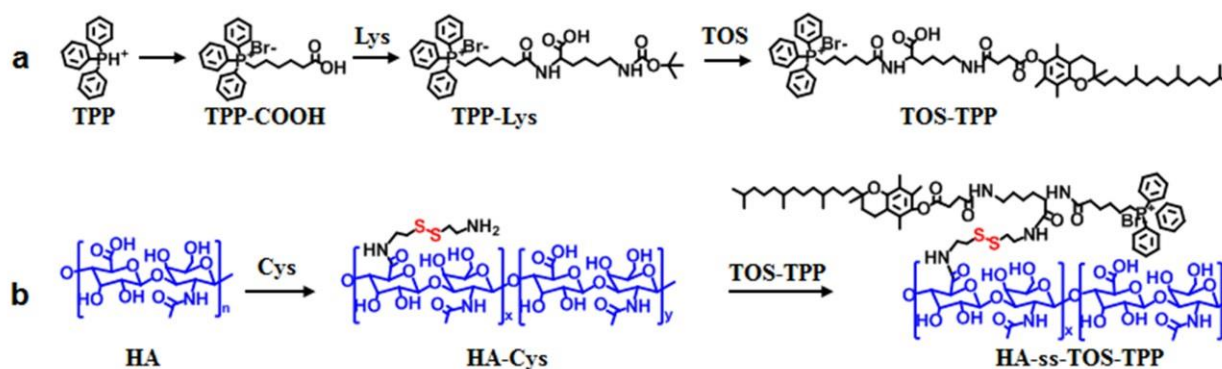
<sup>b</sup> *College of Chemical Engineering, Huaqiao University, Xiamen 361021, P.R. China.*

\* Corresponding author. School of Materials Science and Engineering, Southwest Jiaotong University, Chengdu 610031, P.R. China. Phone: +8628-87634068; fax: +8628-87634649.

E-mail Address: [xhli@swjtu.edu.cn](mailto:xhli@swjtu.edu.cn)

## S1. Materials

Hyaluronic acid (HA, *Mw*: 9.8 kDa) was purchased from the Freda Biochem Co., Ltd. (Shandong, China), and camptothecin (CPT) was from Knowshine Pharmaceuticals Inc. (Shanghai, China). Cystamine, lysine,  $\alpha$ -tocopherylsuccinate (TOS), triphenylphosphonium (TPP), 3,3'-dithiodipropionic acid (DTPA), 1-ethyl-3(3-dimethylaminopropyl) carbodiimide (EDC), *N,N*-dicyclohexylcarbodiimide (DCC), 4-dimethylamino-pyridine (DMAP), and *N*-hydroxysuccinimide (NHS) were used as received from Aladdin (Beijing, China). Trifluoroacetic acid, stannous 2-ethylhexanoate, dialysis bags, deuterated dimethyl sulfoxide (DMSO-*d*<sub>6</sub>) and water (D<sub>2</sub>O) were procured from Sigma (St. Louis, MO). All other chemicals were of analytical grade and obtained from Changzheng Regents Company (Chengdu, China), unless otherwise indicated. Pyridine was dried over CaH<sub>2</sub> and dichloromethane with 4 Å molecular sieves, and distilled prior to use.



**Scheme S1.** (a) Synthetic process of TOS-TPP by coupling of TPP-COOH with TOS via lysine linkers. (b) Synthesis routes for HA-ss-TOS-TPP and (c) HA-ss-TOS by conjugation of TOS and TOS-TPP with HA using cystamine as disulfide linkers.

## S2. Synthesis of TOS-TPP

Scheme S1a illustrates the synthesis process of TOS-TPP by coupling of TPP-COOH with TOS via lysine linkers. TPP-COOH were obtained by reaction of 6-bromohexanoic acid with TPP cations as described previously [1]. Briefly, 6-bromohexanoic acid (500 mg, 2.6 mmol) and triphenylphosphine (700 mg, 2.7 mmol) were dissolved in 15 mL of acetonitrile, followed by refluxation under argon for 24 h. After concentration under reduced pressure, the resulting viscous oil was washed with hexanes and diethyl ether to give a white solid of TPP-COOH. Yield: 86.4%. The <sup>1</sup>H NMR spectrum was

recorded on a Bruker AM 400 apparatus, using tetramethylsilane (TMS) as the internal reference.  $^1\text{H}$  NMR (DMSO- $d_6$ , ppm,  $\delta$ ): 7.8–7.6 ( $-\text{C}_6\text{H}_5$ ), 3.52 ( $-\text{CH}_2-$ ), 2.3 ( $-\text{CH}_2-\text{C}=\text{O}$ ), 1.61 ( $(-\text{CH}_2)_3$ ) (Fig. S1a).

Lysine was linked on TPP-COOH *via* DCC/NHS chemistry to obtain TPP-Lys-NH $_2$ . Briefly, TPP-COOH (457 mg, 1 mmol) was dissolved in 10 mL of dichloromethane, followed by the addition of DCC (216 mg, 1.05 mmol) and NHS (230 mg, 2 mmol) in 5 mL of dichloromethane under stirring. After reaction for 24 h and filtration to remove the formed dicyclohexylurea, the activated TPP (TPP-NHS) was added in 10 mL of DMSO containing BOC-Lys (295 mg, 1.2 mmol). After reaction for 24 h and concentration under reduced pressure, the subsolid was washed with water and filtered to give a white solid of TPP-Lys(BOC). Yield: 73.5%.  $^1\text{H}$  NMR (DMSO- $d_6$ , ppm,  $\delta$ ): 7.8–7.6 ( $-\text{C}_6\text{H}_5$ ), 3.72 ( $-\text{CH}_2-$ ), 2.14 ( $-\text{CH}_2-\text{C}=\text{O}$ ), 1.61 ( $(-\text{CH}_2)_3$ ), 1.37 ( $-\text{CH}_3$ ), 1.29 ( $-\text{CH}_2-$ ), 1.89 ( $-\text{CH}_2-$ ), 3.02 ( $-\text{N}-\text{CH}_2-$ ), 4.23 ( $-\text{CH}(\text{N})-\text{C}-$ ), 7.38 ( $-\text{C}-\text{NH}-\text{C}$ ) (Fig. S1b).

To remove the protection groups, TPP-Lys(BOC) was dissolved in dichloromethane, followed by adding dropwise trifluoroacetic acid (3 mL) under argon. After reaction for 2 h and concentration under reduced pressure, the white solid was washed with diethyl ether to obtain TPP-Lys-NH $_2$ . Yield: 83.7%.  $^1\text{H}$ -NMR (DMSO- $d_6$ , ppm):  $\delta$  7.8–7.6 ( $-\text{C}_6\text{H}_5$ ), 3.52 ( $-\text{CH}_2-$ ), 2.3 ( $-\text{CH}_2-\text{C}=\text{O}$ ), 1.61 ( $(-\text{CH}_2)_3$ ), 1.27 ( $-\text{CH}_2-$ ), 1.65 ( $-\text{CH}_2-$ ), 4.21 ( $-\text{N}-\text{CH}(\text{C}=\text{O})-$ ) (Fig. S1c).

TOS was conjugated with TPP-Lys *via* DCC/NHS chemistry to obtain TOS-TPP. Briefly, TOS (530 mg, 1 mmol) were dissolved in 20 mL of dichloromethane, followed by adding DCC (216 mg, 1.05 mmol) and NHS (138 mg, 1.2 mmol) in 5 mL of dichloromethane under stirring. After reaction for 24 h and filtration to remove dicyclohexylurea, the activated TOS (TOS-NHS) was added dropwise into 20 mL of dichloromethane containing TPP-Lys-NH $_2$  (585 mg, 1 mmol). After reaction for 24 h, the solution was concentrated under reduced pressure and precipitated with diethyl ether to give a white solid of TOS-TPP. Yield: 89.8%.  $^1\text{H}$ -NMR (DMSO- $d_6$ , ppm,  $\delta$ ): 7.8–7.6 ( $-\text{C}_6\text{H}_5$ ), 3.52 ( $-\text{CH}_2-$ ), 2.3 ( $-\text{CH}_2-\text{C}=\text{O}$ ), 1.61 ( $(-\text{CH}_2)_3$ ), 0.87 ( $-\text{CH}_3$ ), 1.90 ( $-\text{CH}_3$ ), 2.78 ( $-\text{CH}_2-$ ), 1.71 ( $-\text{CH}_2-$ ), 1.12 ( $-\text{CH}_2-$ ), 4.19 ( $-\text{N}-\text{CH}(\text{C}=\text{O})-$ ) (Fig. S1d).

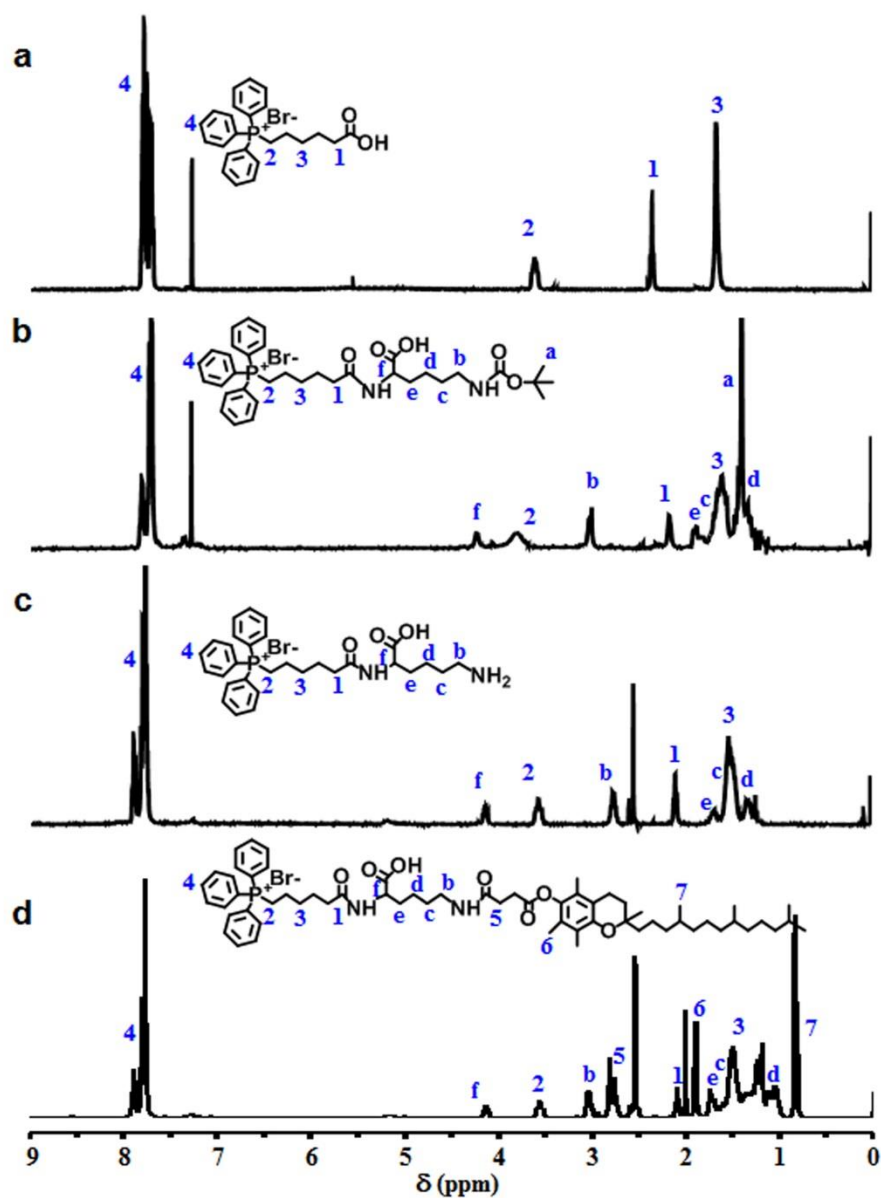


**Fig. S1.**  $^1\text{H}$ -NMR spectra of TPP-COOH (a), TPP-Lys(BOC) (b), TPP-Lys-NH<sub>2</sub> (c) and TOS-TPP (d).

### S3. Synthesis of HA-ss-TOS-TPP

TOS-TPP were conjugated on HA using cystamine as disulfide linkers to obtain HA-ss-TOS-TPP, (Scheme S1b). Cystamine was conjugated onto HA via EDC/NHS activation to introduce disulfide and amino groups into HA-Cys as described before [2]. Briefly, HA (200 mg, 0.5 mmol) was dissolved in 50 mL of phosphate buffered solution (PBS, pH 7.4), followed by adding EDC (77 mg, 0.40 mmol) and

sulfo-NHS (87 mg, 0.40 mmol). Then cystamine dihydrochloride (1.12 g, 5.0 mmol) was added and the reaction mixture was incubated for 4 h at 25 °C under stirring. The resulting solution was dialyzed (2.5 kDa cutoff) against 0.1 M NaCl and then distilled water to remove unreacted cystamine, EDC and sulfo-NHS coupling agents, followed by freeze drying to obtain HA-Cys. Yield: 72.8%.  $^1\text{H-NMR}$  ( $\text{D}_2\text{O}$ , ppm,  $\delta$ ): 1.89 (-CH<sub>3</sub>), 2.91 (-S-S-CH<sub>2</sub>-) (Fig. S2a).

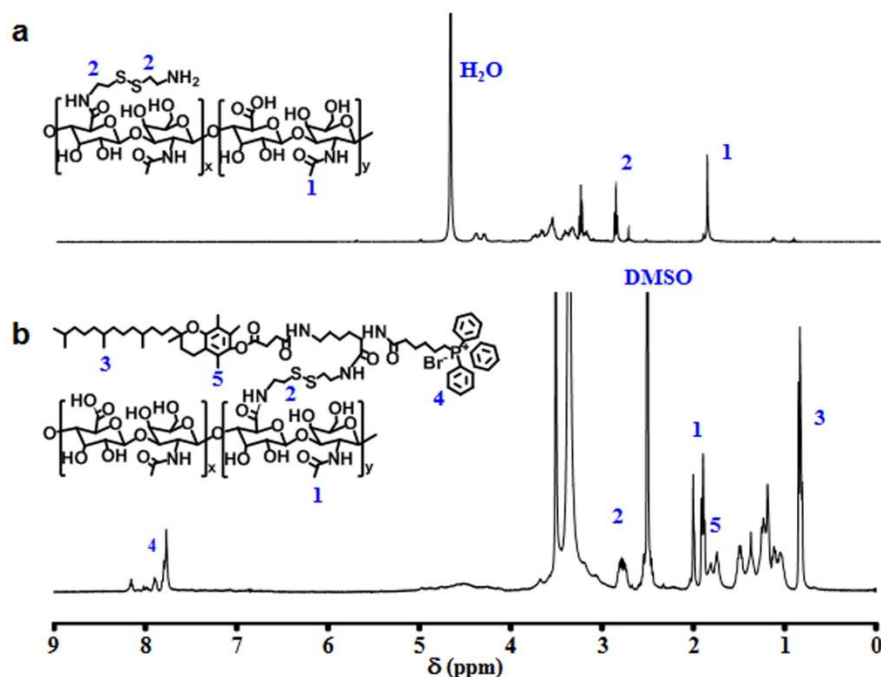


**Fig. S2.**  $^1\text{H-NMR}$  spectra of HA-Cys (a) and HA-ss-TOS-TPP (b).

TOS-TPP was conjugated with HA-Cys via DCC/NHS activation. Briefly, carboxyl groups of TOS-TPP (325 mg, 0.3 mmol) were activated by DCC (72 mg, 0.35 mmol) and NHS (46 mg, 0.4 mmol) in dimethyl formamide at 0 °C for 4 h then at 20 °C for 20 h. The activated TOS-TPP was added dropwise into HA-Cys (220 mg, 0.5 mmol) solution of dimethyl formamide and the reaction was proceeded for 24 h at room temperature with agitation. The resulting solution was dialyzed against DMSO/ethanol (3:1, v/v) for 2 days and distilled water for 2 days, followed by freeze drying to obtain HA-ss-TOS-TPP. Yield: 84.6%.  $^1\text{H NMR}$  ( $\text{D}_2\text{O}/\text{DMSO-}d_6$ , ppm,  $\delta$ ): 7.8–7.6 (-C<sub>6</sub>H<sub>5</sub>), 2.85 (-S-S-CH<sub>2</sub>-), 1.89 (-CH<sub>3</sub>-), 1.78 (-CH<sub>3</sub>-), 0.89 (-CH<sub>3</sub>-) (Fig. S2b). The substitution degree of TOS in HA-ss-TOS-TPP conjugates was determined from the integral ratios of methyl protons of TOS to those of acetyl methyl protons of HA as shown in  $^1\text{H-NMR}$  spectra.

#### S4. Preparation of PLA-cdm-M<sub>T</sub>

Micelle carriers of M<sub>C</sub> and M<sub>T</sub> were conjugated with poly(DL-lactide) (PLA) via acid-labile 2-propionic-3-methylmaleic anhydride (CDM) linkers to obtain PLA-cdm-M<sub>C</sub> and PLA-cdm-M<sub>T</sub> as described previously [3]. CDM was prepared from  $\alpha$ -ketoglutaric acid, and CDM-modified PLA (PLA-cdm) was prepared by acylation of amine-terminated polylactide (PLA-NH<sub>2</sub>) with CDM. PLA-NH<sub>2</sub> was synthesized by sequential tert-butyl-N-(3-hydroxypropyl) carbamate-initiated bulk ring-opening polymerization of DL-lactide and deprotection of Boc groups at the end of the polymer chain [4]. PLA-cdm-M<sub>C</sub> or PLA-cdm-M<sub>T</sub> were synthesized by conjugation of amine-terminated M<sub>C</sub> or M<sub>T</sub> onto PLA-cdm by standard EDC/NHS chemistry. <sup>1</sup>H-NMR (DMSO-*d*<sub>6</sub>, ppm,  $\delta$ ) of PLA-cdm-M<sub>T</sub>: 0.92 (-CH<sub>3</sub>), 1.55 (-CH<sub>3</sub>), 1.85 (-COCH<sub>3</sub>), 5.16 (C-CH-O), 7.87 (-C<sub>6</sub>H<sub>5</sub>) (Fig. S3a). <sup>1</sup>H-NMR (DMSO-*d*<sub>6</sub>, ppm,  $\delta$ ) of PLA-cdm-M<sub>C</sub>: 0.89 (-CH<sub>3</sub>), 1.55 (-CH<sub>3</sub>), 1.85 (-COCH<sub>3</sub>), 1.30–1.36 (-CH<sub>2</sub>-CH<sub>2</sub>-), 1.53 (-CH<sub>2</sub>-), 1.47 (-CH<sub>3</sub>), 5.16 (C-CH-O), 8.70 (=CH-), 8.08–8.19 (=CH-), 7.87 (=CH-), 7.72 (=CH-), 7.19 (=CH-) (Fig. S3b).

#### References

- [1] S. Marrache, S. Dhar, The energy blocker inside the power house: Mitochondria targeted delivery of 3-bromopyruvate, *Chem. Sci.* 6 (2015) 1832–1845.
- [2] J. Li, M. Huo, J. Wang, J. Zhou, J. Mohammad, Y. Zhang, et al, Redox-sensitive micelles self-assembled from amphiphilic hyaluronic aciddeoxycholic acid conjugates for targeted intracellular delivery of paclitaxel, *Biomaterials* 33 (2012) 2310–2320
- [3] Z. Chen, W. Liu, L. Zhao, S. Xie, M. Chen, T. Wang, X. Li, Acid-labile degradation of injectable fiber fragments to release bioresorbable micelles for targeted cancer therapy, *Biomacromolecules* 19 (2018) 1100–1110.
- [4] M. Ju, F. Gong, S. Cheng, Y. Gao, Fast and convenient synthesis of amine-terminated polylactide as a macroinitiator for  $\omega$ -benzyloxycarbonyl-L-lysine-N-carboxyanhydrides, *Int. J. Polym. Sci.* 2011 (2011) 1–7.

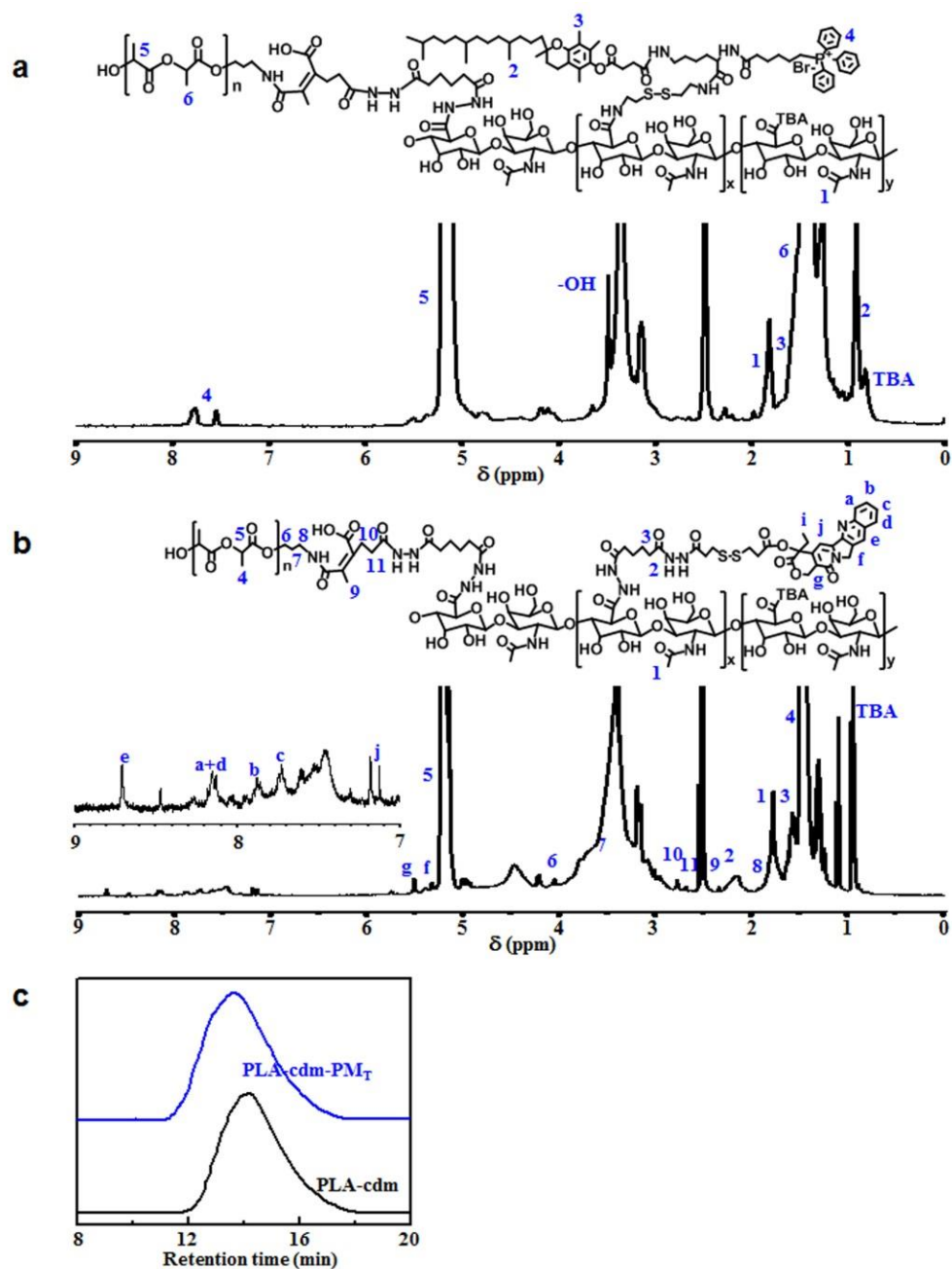


**Fig. S3.**  $^1\text{H}$ -NMR spectra of PLA-cdm-PM<sub>T</sub> (a) and PLA-cdm-PM<sub>C</sub> (b) and the GPC elution profiles of PLA-cdm-PM<sub>T</sub> and PLA-cdm (c).

### S5. CMC determination of micelles

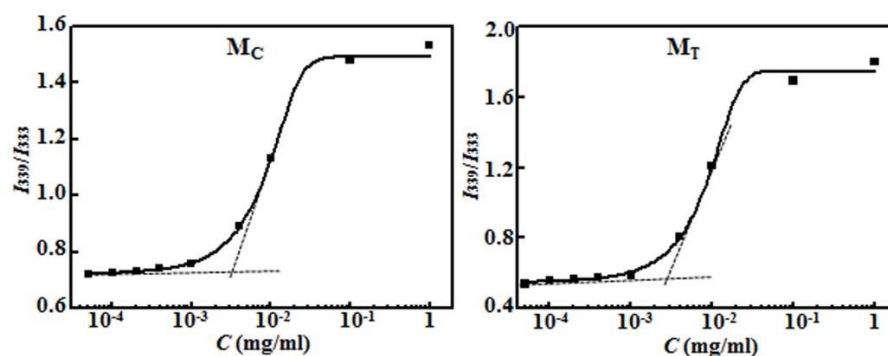


**Fig. S4.**  $I_{339}/I_{333}$  band intensity ratios of pyrene as a function of logarithm concentrations of  $M_C$  and  $M_T$  micelles.

### S6. Cellular uptake of hybrid micelles

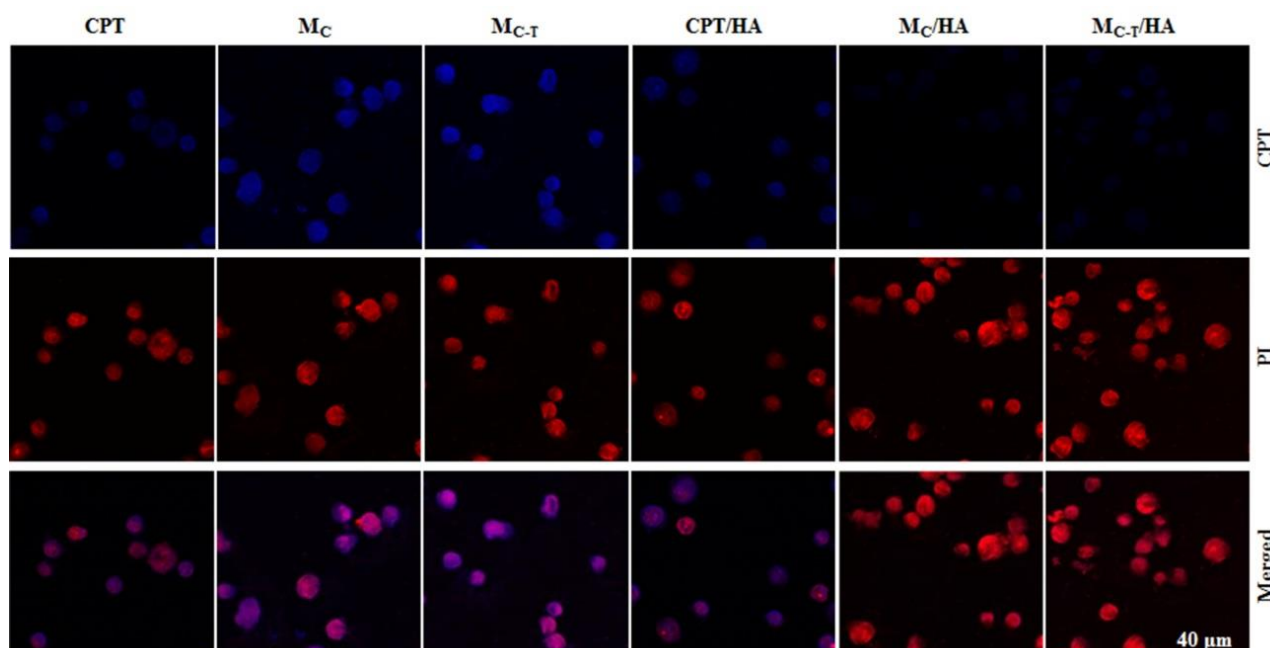


**Fig. S5.** Typical CLSM images of H22 cells, counterstained by propidium iodide after incubation with free CPT,  $M_C$  and  $M_{C-T}$  micelles, compared with the addition of free HA in the media.



*S7. ROS production after treatment with hybrid micelles*

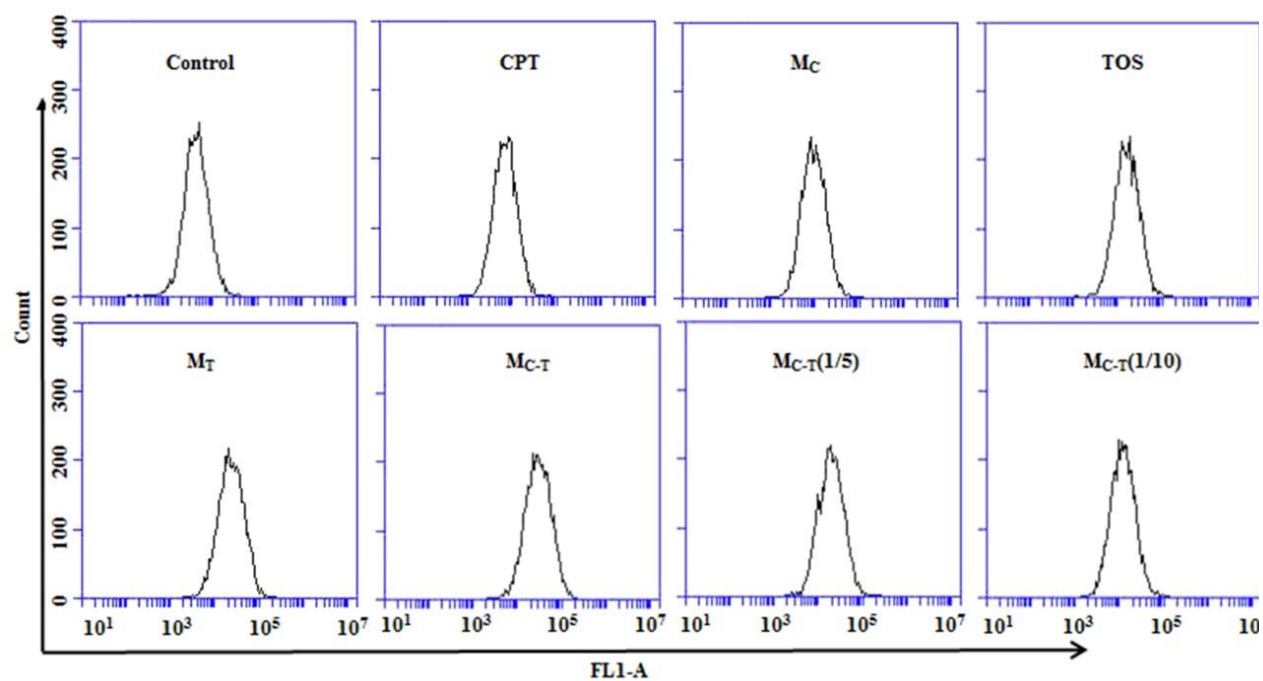


**Fig. S6.** Flow cytometry analysis of intracellular ROS production in H22 cells after incubation with PBS, CPT, TOS,  $M_C$ ,  $M_T$ ,  $M_{C-T}$ ,  $M_{C-T}(1/5)$  and  $M_{C-T}(1/10)$ , using no treatment as control.

S8. Cell apoptosis and life-cycle analysis after treatment with hybrid micelles

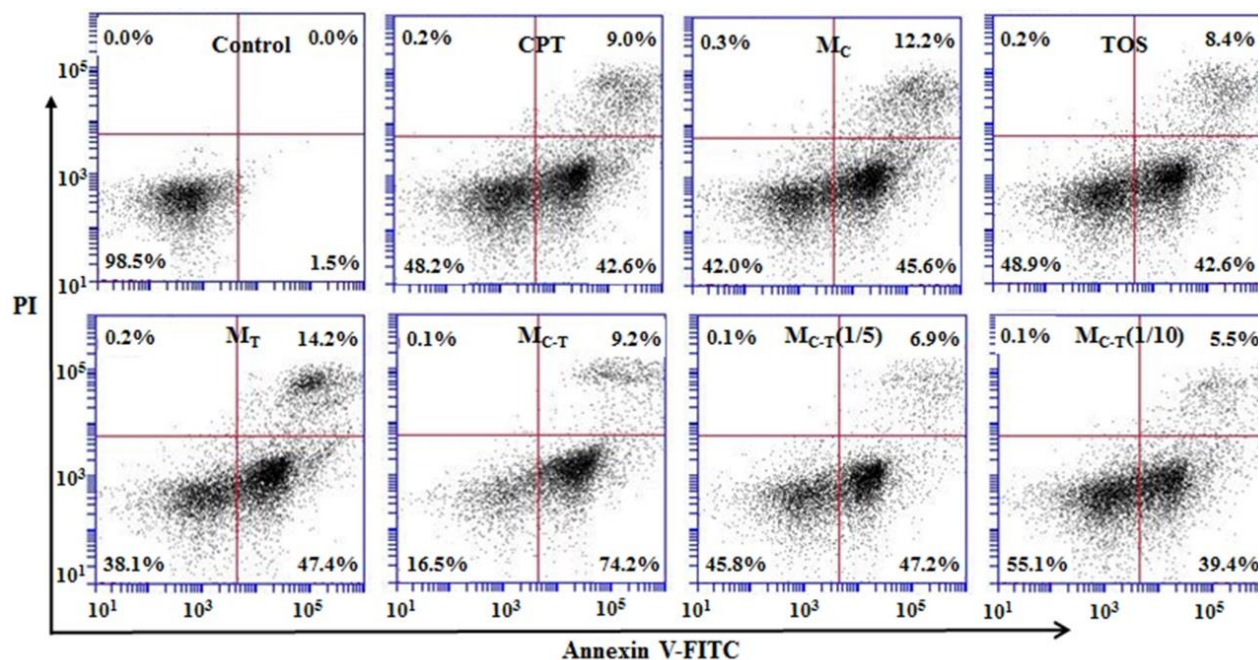


**Fig. S7.** Flow cytometry analysis of H22 cells after incubation for 48 h with free CPT, TOS, M<sub>C</sub>, M<sub>T</sub>, M<sub>C-T</sub>, M<sub>C-T</sub>(1/5) and M<sub>C-T</sub>(1/10), using no treatment as control. Lower left of each image, living cells; Lower right, early apoptotic cells; Upper right, late apoptotic cells; Upper left, necrotic cells. Inserted numbers in each area indicate the percentage of cells present in this area.

*S9. In vivo antitumour efficacy of hybrid micelles*

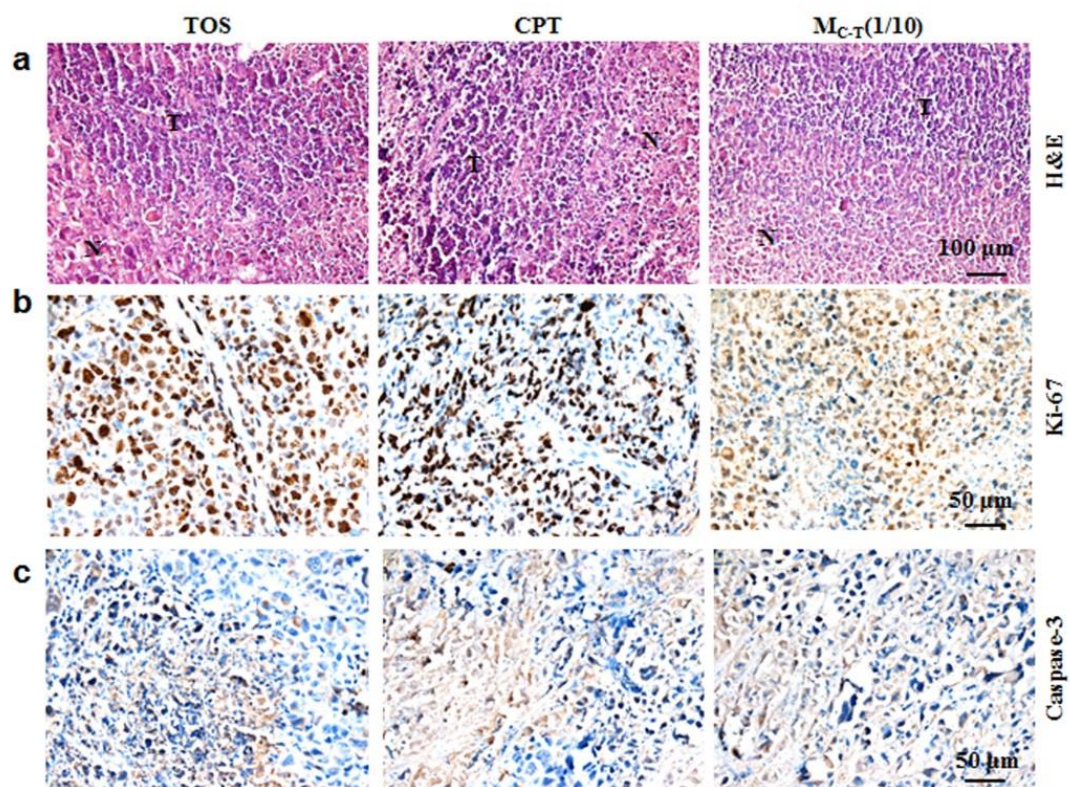


**Fig. S8.** (a) Typical H&E staining images, (b) IHC staining images of Ki-67 and (c) caspase-3 of tumors retrieved on day 21 after intravenous administration of free CPT, TOS and  $M_{C-T}(1/10)$ .



# S10. Systemic toxicity of hybrid micelle treatment

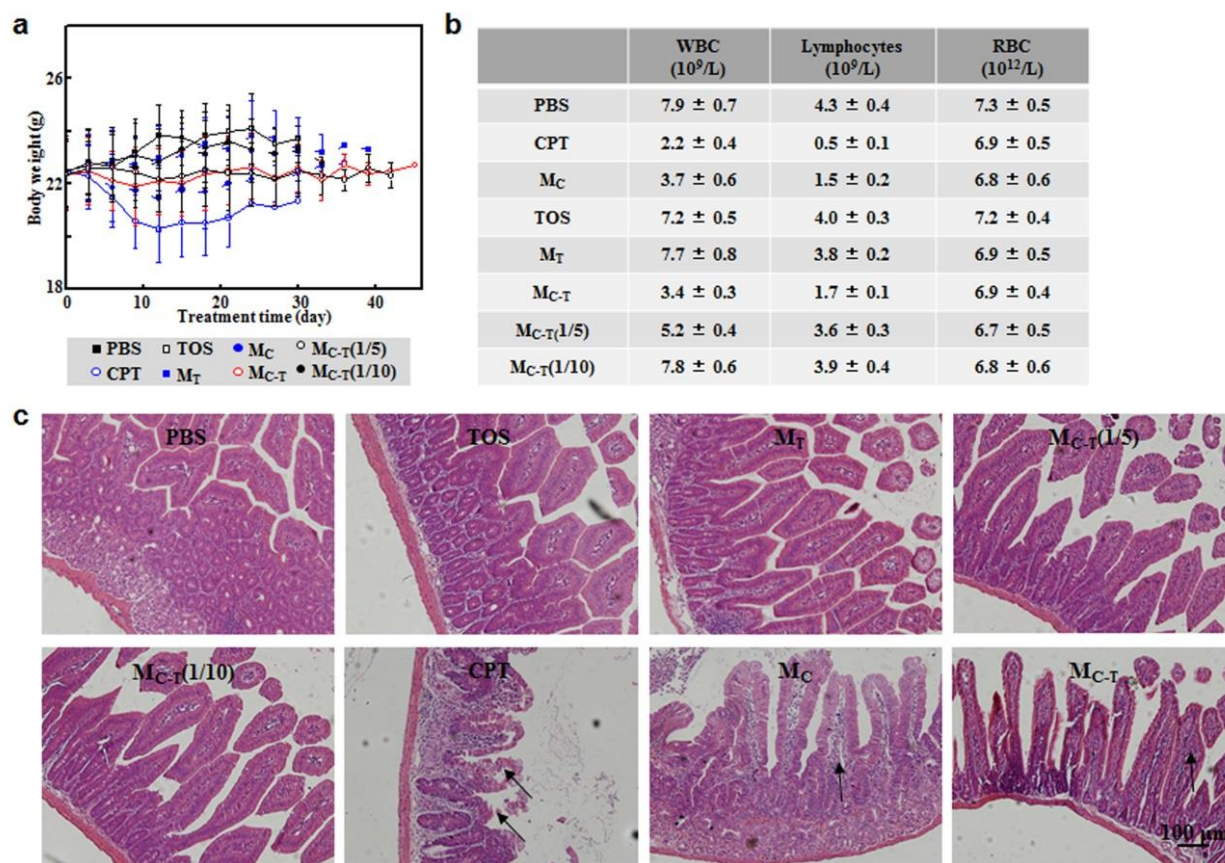


**Fig. S9.** (a) Body weight changes of H22 tumor-bearing mice, (b) WBC, RBC and lymphocyte numbers in blood of mice, (c) typical H&E staining images of small intestines retrieved from tumor-bearing mice after intravenous administration of free CPT, TOS,  $M_C$ ,  $M_T$ ,  $M_{C-T}$ ,  $M_{C-T}(1/5)$  and  $M_{C-T}(1/10)$ , using saline injection as control ( $n = 8$ ). Arrows indicate irregular villi and shrunk crypts.

S11. Characterization of micelle-conjugated short fibers

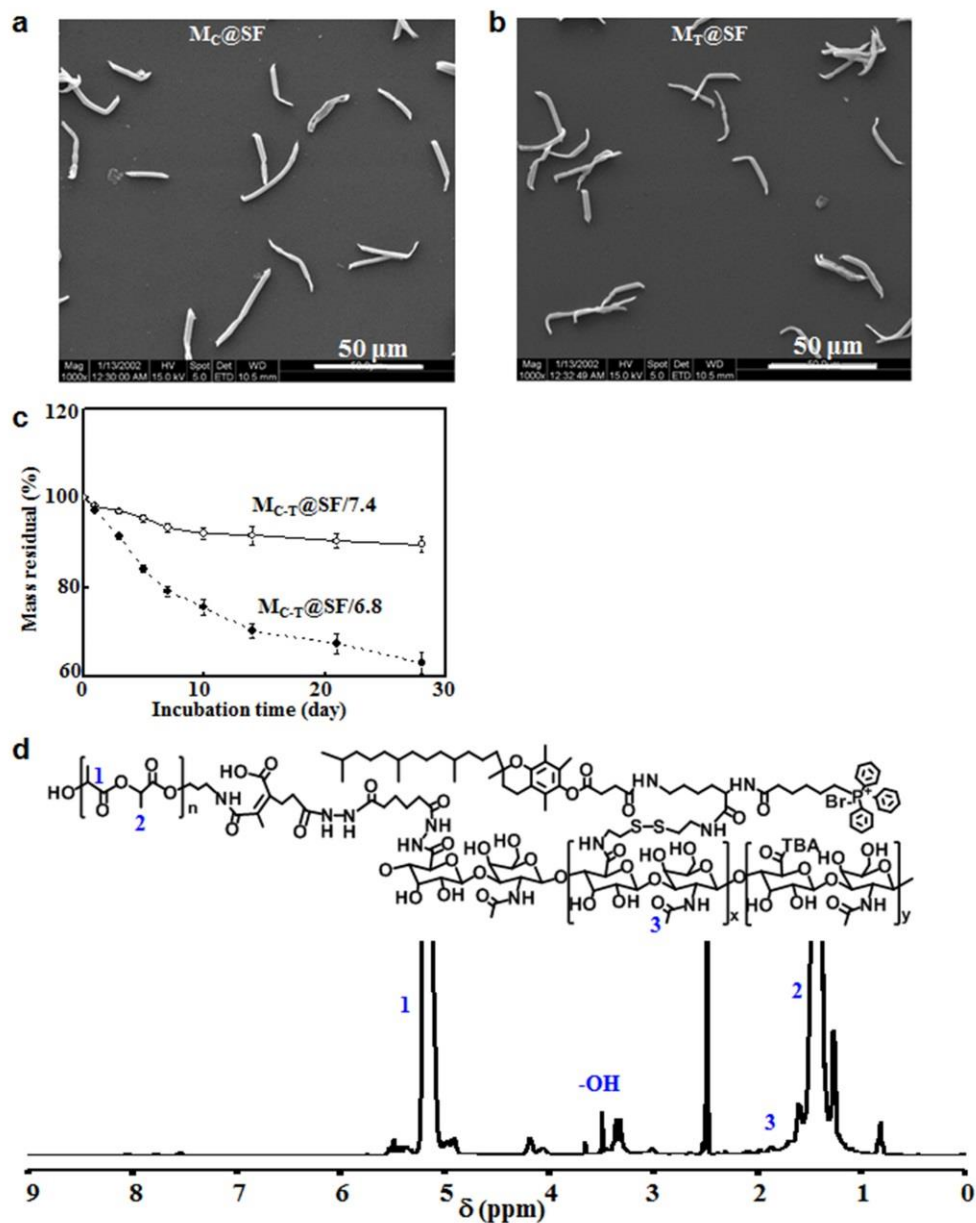


**Fig. S10.** SEM morphologies of  $M_C@SF$  (a) and  $M_T@SF$  (b). (c) Mass loss of  $M_{C-T}@SF$  after incubation at 37  $^{\circ}C$  in pH 7.4 and 6.8 buffers ( $n = 3$ ). (d)  $^1H$  NMR spectrum of  $M_T@SF$  retrieved after incubation at 37  $^{\circ}C$  in pH 6.8 buffers for 28 days.

S12. Characterization of micelles released from short fibers

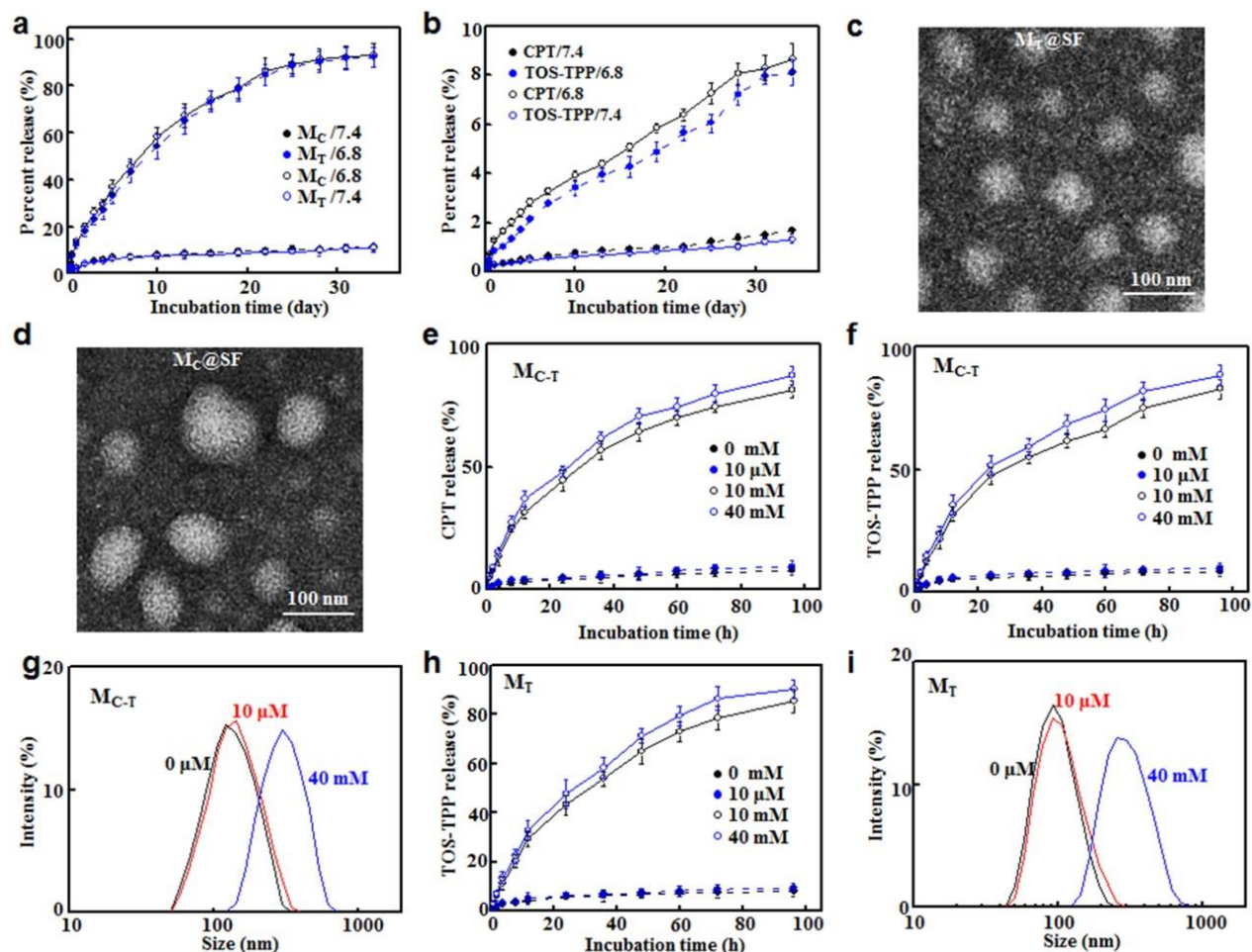


**Fig. S11.** (a) Percent release of  $M_C$  and  $M_T$ , (b) CPT and TOS-TPP from  $M_C$ @SF and  $M_T$ @SF after incubation in pH 7.4 and 6.8 buffers at 37  $^{\circ}$ C ( $n = 3$ ). (c) Typical TEM images of  $M_T$  released from  $M_T$ @SF and (d)  $M_C$  released from  $M_C$ @SF. (e) Percent release of CPT and (f) TOS-TPP from the retrieved  $M_{C-T}$  after incubation in PBS and PBS containing 10  $\mu$ M, 10 and 40 mM GSH at 37  $^{\circ}$ C ( $n = 3$ ). (g) Typical DLS images of the released  $M_{C-T}$  after incubation in PBS and PBS containing 10  $\mu$ M, 10 and 40 mM GSH at 37  $^{\circ}$ C for 24 h. (h) Percent release of TOS-TPP from the retrieved  $M_T$  after incubation in PBS and PBS containing 10  $\mu$ M, 10 and 40 mM GSH at 37  $^{\circ}$ C ( $n = 3$ ). (i) Typical DLS images of the retrieved  $M_T$  micelles after incubation in PBS and PBS containing 10  $\mu$ M, 10 and 40 mM GSH at 37  $^{\circ}$ C for 24 h.



*S13. In vivo antitumor efficacy of short fibers*

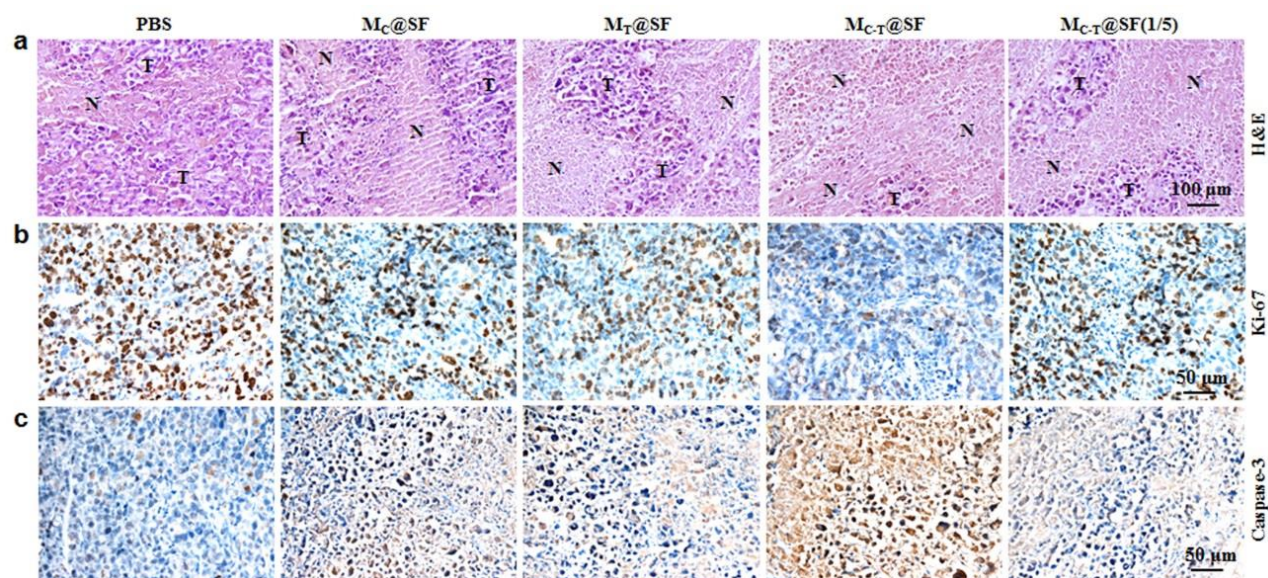


**Fig. S12.** (a) Typical H&E staining images ("N" represents necrotic area, "T" represents tumor mass), (b) IHC staining images of Ki-67 and (c) caspase-3 of tumors retrieved on day 21 after intratumoral administration of  $M_C@SF$ ,  $M_T@SF$ ,  $M_{C-T}@SF$  and  $M_{C-T}@SF(1/5)$ , using saline injection as control.